

# Multi-scale species richness estimation with deep learning

Victor Boussange<sup>1,\*</sup>, Bert Wuyts<sup>1</sup>, Philipp Brun<sup>1</sup>, Johanna T. Malle<sup>1,2</sup>, Gabriele Midolo<sup>3</sup>, Jeanne Portier<sup>4</sup>, Théophile Sanchez<sup>5,6</sup>, Niklaus E. Zimmermann<sup>1</sup>, Irena Axmanová<sup>7</sup>, Helge Bruelheide<sup>8,9</sup>, Milan Chytrý<sup>7</sup>, Stephan Kambach<sup>8</sup>, Zdeňka Lososová<sup>7</sup>, Martin Večeřa<sup>7</sup>, Idoia Biurrun<sup>10</sup>, Klaus T. Ecker<sup>11</sup>, Jonathan Lenoir<sup>12</sup>, Jens-Christian Svenning<sup>13</sup>, Dirk Nikolaus Karger<sup>1</sup>

<sup>1</sup> Dynamic Macroecology, Land Change Science, Swiss Federal Research Institute WSL, CH-8903 Birmensdorf, Switzerland

<sup>2</sup> Department of Evolutionary Biology and Environmental Studies, University of Zurich, Zurich, Switzerland

<sup>3</sup> Department of Spatial Sciences, Faculty of Environmental Sciences, Czech University of Life Sciences Prague, Praha - Suchbát, Czech Republic

<sup>4</sup> Resource Analysis, Forest Resources and Management, Swiss Federal Research Institute WSL, CH-8903 Birmensdorf, Switzerland

<sup>5</sup> Ecosystems and Landscape Evolution, Department of Environmental Systems Science, ETH Zürich, Zürich, Switzerland

<sup>6</sup> Ecosystems and Landscape Evolution, Land Change Science, Swiss Federal Research Institute WSL, CH-8903 Birmensdorf, Switzerland

<sup>7</sup> Department of Botany and Zoology, Faculty of Science, Masaryk University, Brno, Czech Republic

<sup>8</sup> Institute of Biology, Geobotany and Botanical Garden, Martin Luther University Halle-Wittenberg, Halle (Saale), Germany

<sup>9</sup> German Centre for Integrative Biodiversity Research (iDiv) Halle-Jena-Leipzig, Leipzig, Germany

<sup>10</sup> Department of Plant Biology and Ecology, Faculty of Science and Technology, University of the Basque Country UPV/EHU, Bilbao, Spain

<sup>11</sup> Ecosystem Dynamics, Biodiversity and Conservation Biology, Swiss Federal Research Institute WSL, CH-8903 Birmensdorf, Switzerland

<sup>12</sup> UMR CNRS 7058 'Ecologie et Dynamique des Systèmes Anthropisés' (EDYSAN), Université de Picardie Jules Verne, F-80037 Amiens, France

<sup>13</sup> Center for Ecological Dynamics in a Novel Biosphere (ECONOVO), Aarhus University, DK-8000 Aarhus C, Denmark

\* Corresponding author, email: vic.boussange@gmail.com

August 21, 2025

## Abstract

Biodiversity assessments are critically affected by the spatial scale at which species richness is measured. How species richness accumulates with sampling area depends on natural and anthropogenic processes whose effects can change depending on the spatial scale considered. These accumulation dynamics, described by the species-area relationship (SAR), are challenging to assess because most biodiversity surveys are restricted to sampling areas much smaller than the scales at which these processes operate. Here, we combine sampling theory and deep learning to predict local species richness within arbitrarily large sampling areas, enabling for the first time to estimate spatial differences in SARs. We demonstrate our approach by predicting vascular plant species richness across Europe and evaluate predictions against an independent dataset of plant community inventories. The resulting model, named deep SAR, delivers multi-scale species richness maps, improving coarse grain richness estimates by 32% compared to conventional methods, while delivering finer grain estimates. Additional to its predictive capabilities, we show how our deep SAR model can provide fundamental insights on the multi-scale effects of key biodiversity processes. The capacity of our approach to deliver comprehensive species richness estimates across the full spectrum of ecologically relevant scales is essential for robust biodiversity assessments and forecasts under global change.

**Significance statement.** Understanding how biodiversity responds to global change requires assessing species richness across spatial scales. Yet, most biodiversity data are collected at local scales, while the ecological processes that shape richness often act regionally or globally. This mismatch makes it difficult to track biodiversity change effectively. Here, we bridge this gap by integrating sampling theory with deep learning to predict species richness across scales. Using ~490k vegetation surveys, we map vascular plant richness across Europe and validate our predictions with independent data. Our model, named deep SAR, improves large-scale richness estimates by 32% compared to standard methods, while revealing the multi-scale nature of biodiversity patterns. This work delivers a scalable framework for monitoring and forecasting biodiversity under global change.

## Contents

<b>1 Introduction</b>	<b>2</b>
<b>2 Results</b>	<b>5</b>
2.1 Model performance . . . . .	5
2.2 Contribution of area and environment across spatial scales . . . . .	6
2.3 Scale-specific patterns of plant species richness and turnover in Europe . . . . .	7
<b>3 Discussion</b>	<b>10</b>
<b>4 Conclusion</b>	<b>11</b>
<b>5 Methods</b>	<b>11</b>
5.1 Estimating total species richness from small samples . . . . .	11
5.2 Deep SAR model . . . . .	13
5.3 Data . . . . .	14
<b>6 Data availability</b>	<b>14</b>
<b>7 Code availability</b>	<b>14</b>
<b>8 Author contributions</b>	<b>14</b>
<b>9 Acknowledgements</b>	<b>14</b>
<b>S1 Supplementary text</b>	<b>21</b>
S1.1 Decomposition of $p_0$ . . . . .	21
<b>S2 Supplementary table</b>	<b>22</b>
<b>S3 Supplementary figures</b>	<b>23</b>

## 1 Introduction

Biodiversity is experiencing unprecedented changes due to global change stressors (IPBES, 2019), with impacts that critically vary across spatial scales (Smart et al., 2006). Agriculture, for example, can increase local diversity through biotic homogenization, but causes biodiversity loss at regional scales by degrading natural habitats (Fahrig, 1997; Maxwell et al., 2016; Simkin et al., 2022; Keil et al., 2015). Similarly, climate change drives divergent richness patterns across spatial scales by altering species distributions and community assembly processes (IPBES, 2019). Assessing how diversity responds to global change across spatial scales is therefore crucial for evaluating the state and trends of biodiversity (Powers and Jetz, 2019; Newbold, 2018; He and Hubbell, 2011; Rahbek, 2005). Yet, scaling up small-scale effects from local to regional levels poses a major challenge, resulting in a critical knowledge gap (IPBES et al., 2018).

The species-area relationship (SAR) is a key concept to comprehend biodiversity patterns across spatial scales. Here, we use the term "spatial scale" broadly to designate the sampling area, study extent, spatial resolution, or spatial grain, *sensu* O'Neill (1986). Traditionally expressed as a power law,  $S = cA^z$  (Arrhenius, 1921), the SAR describes how species richness  $S$  increases with sampling area  $A$ . The parameter  $c$  represents the species richness observed within a unit area, commonly referred to as  $\alpha$ -diversity.  $z$  determines the slope of the SAR on a log-log scale (i.e., the derivative of  $\log S$  w.r.t  $\log A$ ), with higher  $z$  values indicating a faster accumulation of species with area.  $z$  is often associated with the concept of  $\beta$ -diversity, or species turnover (see Matthews et al. (2021a); Halley et al. (2013); Whittaker and Fernández-Palacios (2007); Triantis et al. (2012), although these terms have alternative definitions (Tuomisto, 2010)). The SAR permits therefore to scale-up local  $\alpha$ -diversity to estimate regional species richness, also known as  $\gamma$ -diversity. By allowing the prediction of biotic diversity across full range of ecologically relevant spatial scales, the SAR is instrumental for a comprehensive estimation of species richness.

While the power-law SAR model is a convenient formulation, it relies on the strong assumption of a linear relationship between area and species richness on a log-log scale, which may be considered only valid for a limited range of scenarios and spatial scales (Dengler, 2009; Guilhaumon et al., 2008). In reality, the accumulation of species richness changes in a non-linear fashion as different environmental drivers and ecological barriers are encountered at increasingly larger spatial extents (Conor and McCoy (2013); Chisholm et al. (2025); Borda-de-Água et al. (2025)). As a consequence, the SAR is also location-specific, and depends on biotic and abiotic factors within the area considered (Betts et al. (2014); Matthews et al. (2016); He and Legendre (2002)). Drivers, such as climate, topography, soil conditions, and habitat type shape the spatial distribution of species, affecting the rate at which they accumulate (He and Legendre, 2002; He and Hubbell, 2011; Weigelt and Kreft, 2013; Matthews et al., 2021b; Chisholm et al., 2025; Borda-de-Água et al., 2025; Ulrich et al., 2022; Drakare et al., 2006). Importantly, the effect of these drivers is also scale dependent (Willis and Whittaker, 2002; Turner and Tjørve, 2005; Wiens, 1989).

A number of studies have characterized the effect of environmental drivers on the SAR (Turner and Tjørve, 2005). One branch of research has relied on exhaustive species inventories from islands or political units to investigate these effects. For instance, Triantis et al. (2003); Kallimanis et al. (2008) showed that incorporating habitat heterogeneity into SAR models better captures spatial variations in species richness, while Kalmar and Currie (2007) extended a power law SAR model by incorporating climate-species interactions to predict global bird species richness. However, the coarse spatial scales of these spatial units limits the characterization of subtle differences in SAR arising at finer spatial grains.

To resolve species richness at finer spatial scales, another line of research has relied on upscaling methods to estimate species richness from partially sampled spatial units (Kunin et al., 2018; Portier et al., 2022; ?). These approaches use sampling theory, which, by making explicit or implicit assumptions about the species density distribution, enable the estimation of the total species richness within the spatial unit considered under asymptotic sampling effort, based on a limited number of small-scale ecological surveys (Chao et al., 2014; Elena Schmitz and Rahmann, 2025). One prominent method involves fitting a parametric function to the species rarefaction curve, which describes how species richness increases with sampling effort within a given spatial unit (see Fig. 1 for an illustration). Unlike the SAR, which typically relates richness to a contiguous area, the rarefaction curve describes how expected richness grows with sampling effort, where samples are not necessarily contiguous. The rarefaction curve is bounded by total species richness within the spatial unit, which can be estimated by extrapolation under asymptotic sampling effort (Soberón M. and Llorente B., 1993; Gotelli and Colwell, 2001). Conditioning this parametric function on the spatial unit's area and associated environmental covariates could theoretically enable the prediction of location- and area-specific rarefaction curves; by extrapolation, it could provide location-specific estimates of species richness for arbitrary spatial grains.

Here, we present a deep learning approach that leverages small-scale ecological surveys and sampling theory to predict spatially explicit SARs. We train a deep neural network to predict the species rarefaction curve expected within a spatial unit based on its area and associated environmental covariates (see Fig. 1 for an illustration). The neural network parametrizes a parametric function that predicts expected species richness for a given sampling effort. By extrapolating this statistical model to its asymptote, we can estimate total species richness within the spatial unit. We formally justify this approach using sampling theory in Methods. Since our model can predict total species richness within spatial units of arbitrary area, we refer to it as a deep SAR model. Using a large dataset of  $\sim 490k$  vegetation plots from the European Vegetation Archive comprising 9,480 distinct species (EVA, Chytrý et al. (2016)), we show how our deep SAR model enables multi-scale estimates of vascular plant species richness

across Europe. We evaluate the model’s interpolation performance using a held-out dataset, and its extrapolation performance using an independent dataset of regional plant inventories from the GIFT database (Weigelt et al., 2020). For environmental features, we calculate the mean and standard deviation of seven bioclimatic variables within each spatial unit, characterizing respectively mean environmental conditions and environmental heterogeneity. We consider three model variants trained using area only, environmental features only, or both, to systematically evaluate their contributions to predicting species richness. We benchmark our deep SAR model against a conventional non-parametric species richness estimator, and employ Shapley value analysis to disentangle how environmental drivers influence species richness across spatial scales. Finally, we demonstrate the model’s capacity to generate spatially explicit maps of plant species richness and turnover across Europe at multiple spatial scales, revealing the multi-scale aspect of biodiversity patterns.

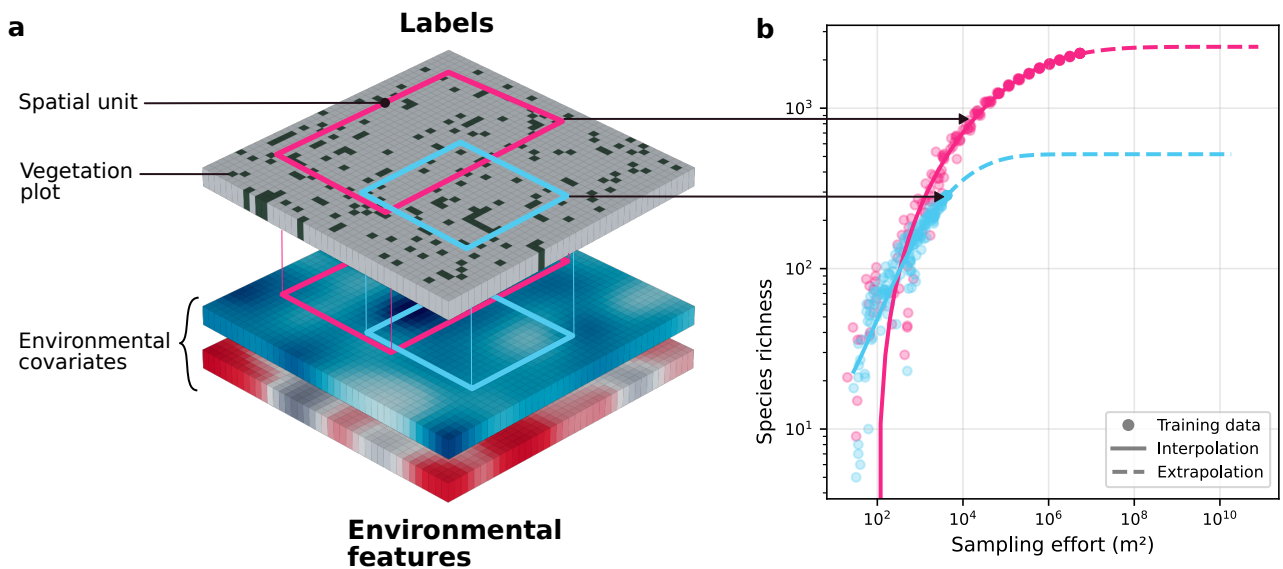


Figure 1: **Deep learning approach for predicting location and area-specific rarefaction curves from small-scale ecological surveys.** (a) Data preparation and feature extraction. The green cells on the top layer correspond to the location of ecological surveys, which are randomly pooled within spatial units of varying sizes and locations (blue and red boxes) to construct location and area-specific rarefaction curves. The bottom layers show environmental covariates, which we use to derive features characterising the spatial units. (b) Location and area-specific species rarefaction estimation. For each spatial unit, subsampled species counts (scatter points) are fitted with an asymptotic statistical model, which we extrapolate to estimate the total expected species richness under infinite sampling effort. We justify this approach with sampling theory (see Methods for details). A deep neural network learns to predict the parameters of this asymptotic statistical model based on the spatial unit environmental features, enabling the estimation of the rarefaction curve for any location and spatial extent, and the prediction of species richness over increasing area. In practice, we only generate one subsampled species count per spatial unit, but many more spatial units, to span large extents efficiently.

## 2 Results

### 2.1 Model performance

Environmental features could significantly improve the estimation of species rarefaction curves (Fig. 2a). We trained three model variants using different sets of features: area only, environmental features only, and both area and environmental features. Using held-out vegetation plots (see Biodiversity data for details on the training and test datasets), we assessed the ability of the models to predict species rarefaction curves across spatial units of varying location and area, for low to moderate sampling effort. Following Kunin et al. (2018), we calculated the root mean squared error (RMSE) of the predictions, measured across five independent training runs. Providing the models with statistics on environmental covariates reduced the RMSE on the EVA test dataset by 43% compared to using area only. The performance of the model informed with both area and environmental features was not significantly improved compared to the model trained with environmental features only. This can be attributed to the high correlation between the standard deviations of environmental features and the spatial unit area (see correlation matrix in Fig. S3). The best models showed a median relative bias of 19% in predicting the species rarefaction curves on the EVA-based test dataset (Fig. 2b), indicating a moderate tendency to overpredict species richness. This bias was more pronounced for low values of species richness and decreased towards 0 as species richness increased (see Fig. S4). This result demonstrates the capability of our approach to resolve fine-grained variations in species rarefaction curves.

The model variant trained with both area and environmental features together demonstrated superior performance in extrapolating to predict total species richness (Fig. 2a). Total species richness was obtained by extrapolating the predicted rarefaction curve towards its asymptote, assuming infinite sampling effort. We matched these predictions against species richness derived from species inventories obtained from the GIFT database. The RMSE of the model trained with area and environmental features was 23% lower than that of the model trained with area only. Contrary to its interpolation performance on the EVA dataset, we found a significant advantage in using area together with environmental features over environmental features only (performance gain of 12%,  $p$ -value  $< 0.001$  under t-test). The improved performance provided by the sampling unit area can be interpreted as an effect of "area-*per se*" (Connor and McCoy, 1979). Along this mechanism, larger areas promote higher species richness independently of environmental niche diversity (Drakare et al., 2006), where increasing area alone allows for more individuals to be sampled and bridging dispersal barriers. We note that the distribution of data points in the GIFT dataset is biased towards larger areas (in the order of magnitude of a country's area, see Fig. S2). At this scale, the summary statistics of environmental features used to inform the model are less informative than for smaller areas (see Contribution of area and environment across spatial scales and Fig. 3), and species richness shows less variation. We expect that more fine-grained species inventories or the use of higher-order summary statistics for the environmental features would give a larger advantage to the model trained with environmental features. It is worth noting that the model significantly outperformed the Chao2 estimator in extrapolation performance, achieving a 32% reduction in RMSE ( $p$ -value  $< 0.001$ , t-test) and providing less biased estimates of species richness (median relative bias of -22% compared to -52% for the Chao2 estimator).

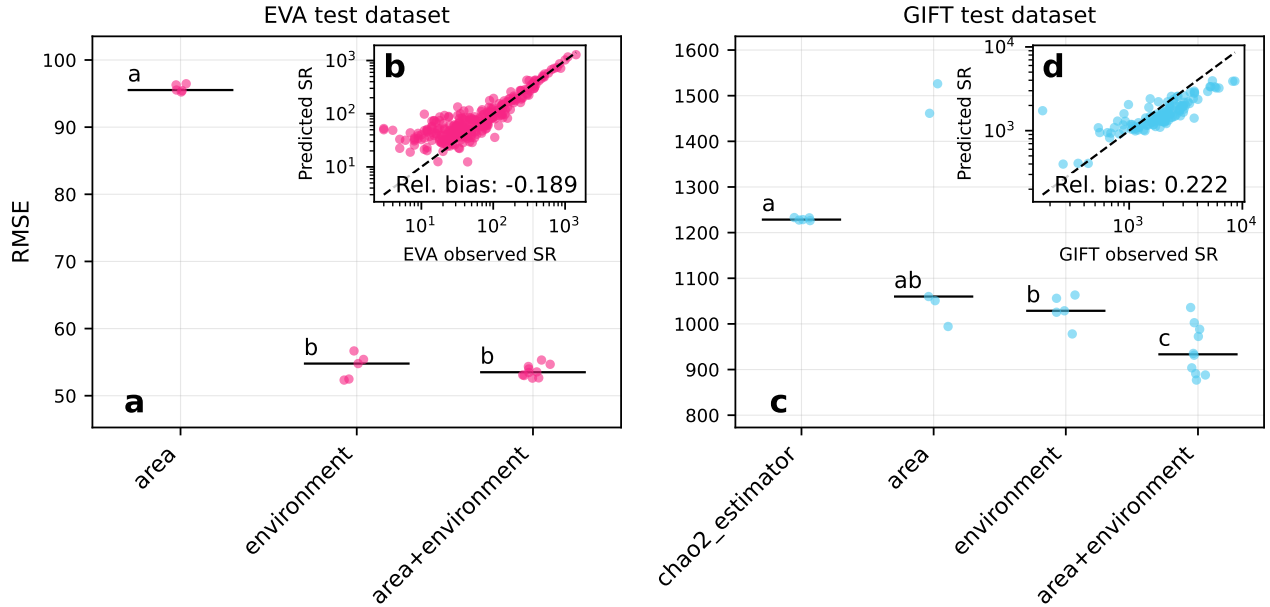


Figure 2: **Ablation study and performance evaluation of the deep SAR model.** (a) Interpolation performance of the model for low to moderate sampling effort, as measured by the root mean squared error (RMSE), trained with each set of features, on the held-out plot vegetation test dataset (EVA test dataset). Different lower letters above the boxplots indicate that performance are significantly different from each other (Posthoc Tukey HSD test). (b) Observed species richness against values predicted by the best model (area + environment). (c) Extrapolation performance of the model, trained with each set of features, and compared against the non-parametric Chao2 estimator, on the species inventories test dataset (GIFT test dataset). (d) Observed species richness against values predicted by the best model (area + environment).

In summary, these results suggest that (i) our model effectively predicts the rarefaction curves associated with spatial units of arbitrary location and extent, providing the expected species richness given a certain sampling effort, and (ii) reliably extrapolates to predict total species richness. As a consequence, the model can predict variations in species richness across locations and spatial scales, capturing location-specific species-area relationships. In the following, we refer to the model trained with area and environmental features as the deep SAR model.

## 2.2 Contribution of area and environment across spatial scales

Disentangling the effect of spatial unit area on species richness from environmentally-related confounding factors has been a challenging task in macroecology, as these factors act differently depending on spatial scale. To quantify the relative contributions of environmental features versus area, we calculated the Shapley values associated with the prediction of total species richness on the EVA test dataset for each predictor class (area of the spatial unit considered, mean and heterogeneity of environmental conditions), stratified by sampling area. Shapley values are commonly used in explainable artificial intelligence to measure the contribution of each feature to the model's output by evaluating all possible feature combinations (Lundberg and Lee, 2017). Specifically, we calculated absolute Shapley values for each predictor class and normalized them so that the sum of Shapley values for all features equals one for each species richness estimates. This approach allowed us to characterize the relative importance of each predictor class across varying sampling areas, as shown in Fig. 3.

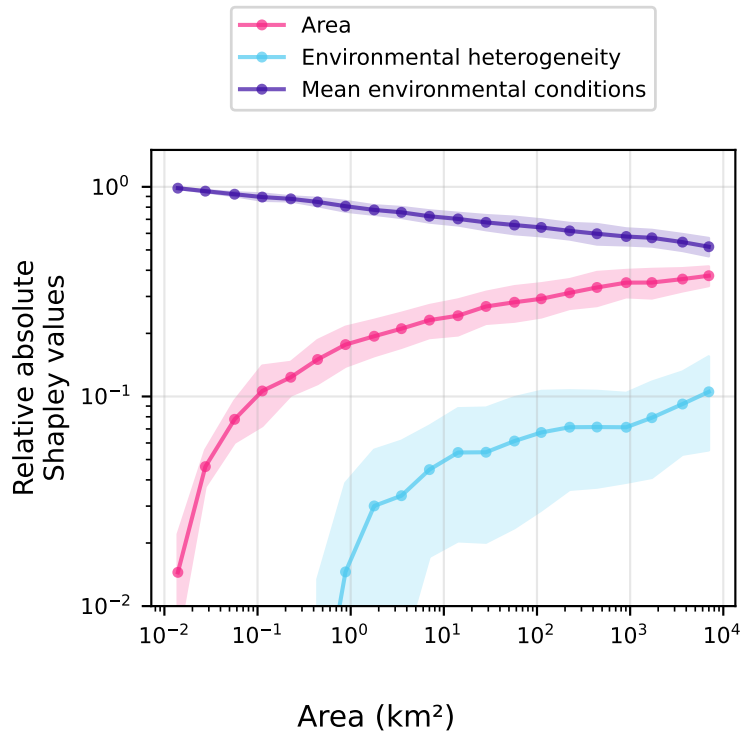


Figure 3: **Relative importance of area and environmental features in predicting total species richness.** Shapley values indicate the contribution of each predictor class, i.e., spatial unit area, mean environmental conditions (mean of environmental covariates), and environmental heterogeneity (standard deviation of environmental covariates), to total species richness estimates at different spatial grains. Lines show mean relative absolute Shapley values; shaded areas show standard deviation.

Mean environmental conditions were contributing the most to species richness predictions across all spatial scales investigated. This finding supports the environmental filtering hypothesis, wherein mean environmental conditions constrain species richness by limiting species establishment based on physiological tolerances (Whittaker, 1972; Vellend, 2010). As the spatial grain increased, the relative contributions of both area and environmental heterogeneity increased, while the contribution of mean environmental conditions decreased. The contribution of spatial unit area was particularly pronounced, with a sustained increase as spatial grain increased, whereas the contribution was overall least pronounced (see Biodiversity data). This finding resonates again with the "area-*per se*" effect (see previous section), where larger areas can support more species simply by providing more space and resources, independent of environmental conditions. Meanwhile, the increasing contribution of environmental heterogeneity at larger spatial grains aligns with the "habitat-diversity hypothesis", wherein environmental heterogeneity promotes higher species richness by increasing niche diversity, which supports greater species turnover (Stein et al., 2014; Qian and Ricklefs, 2012; Turner and Tjørve, 2005). We note that environmental heterogeneity naturally began to rise only at spatial grains larger than the environmental covariate resolution; using environmental covariates with a finer resolution would likely change this pattern. Overall, these findings illustrate the scale-dependent nature of biodiversity drivers (Rahbek, 2005) and help quantify the relative contributions of mechanisms underlying species richness patterns across spatial scales (Field et al., 2009).

### 2.3 Scale-specific patterns of plant species richness and turnover in Europe

Projections of species richness and turnover across spatial scales are essential for comparing biodiversity trends from local to regional levels. Here we used our deep SAR model to map species richness and turnover across Europe at multiple spatial scales. We defined turnover as the slope of the SAR predicted at each location ( $\frac{dS}{dA}(A)$ ). Using a moving window approach with different spatial grains, we derived environmental features that served as predictors to estimate species richness within each window. We also estimated location-specific SARs for three environmentally distinct locations by incrementally increasing the area of spatial units centered at each location of interest.

The model revealed markedly different patterns of species richness across spatial scales. At fine spatial scales (1 km), mountainous areas exhibited relatively lower species richness compared to lowland regions (Fig. 4b), contrary to

established biogeographical knowledge of European vascular plant diversity (Cai et al., 2023). However, predictions at coarser spatial scales (50 km) revealed the expected highest species richness along the Mediterranean coastline and in mountainous regions including the Alps, Carpathians, and Dinarides (Fig. 4c). This scale-dependent variation underscores the critical importance of considering spatial grain in macroecological analyses (Wiens, 1989; Portier et al., 2022).

The predicted location-specific SARs explicitly embed these scale-dependent dynamics (Fig. 4a). The Southwestern Alps (blue curve) exhibited lower local species richness at fine spatial scales compared to the Northern Iberian Peninsula (purple curve) and Northern Germany (red curve). However, as spatial scale increases, species richness in the Alps surpasses both other locations due to higher species turnover. This pattern reflects the characteristic biodiversity structure of mountain environments, where lower local carrying capacity is offset by higher niche diversity driven by environmental heterogeneity, resulting in low local richness but high species turnover and regional richness (Antonelli et al., 2018). The geographic variations in species turnover reflected these patterns (Fig. 4d-e). Notably, turnover patterns differed substantially from species richness patterns at fine scales. Mountain environments showed moderate species richness but high turnover, which effectively translated into higher species richness at coarser scales.

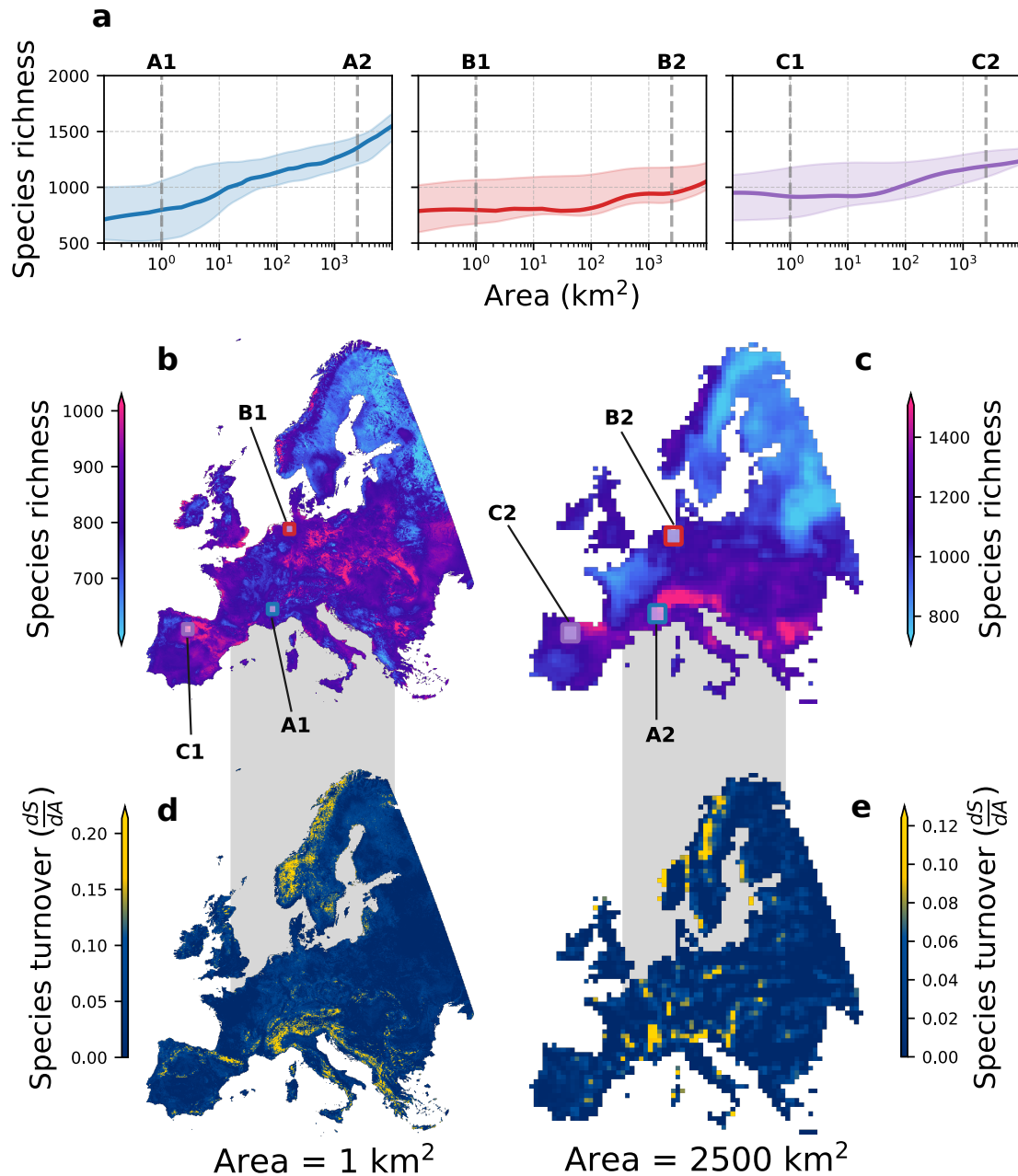


Figure 4: **Species richness and turnover across Europe, predicted at multiple spatial scales.** (a) Predicted SARs for three distinct locations, as indicated in panels (b) and (c). Plain lines represent the mean while shaded areas indicate the standard deviation of the predictions derived from the ensemble model. (b-c) Maps of species richness obtained for square spatial units with edge lengths of 1 km and 50 km, respectively. (d-e) Associated maps of species turnover. Species turnover is defined as the slope of the SAR predicted at each location.

### 3 Discussion

In this work, we demonstrated how deep learning combined with sampling theory enables spatially explicit prediction of species richness from fine to coarse spatial grains. Our deep SAR model learns species rarefaction curves conditioned on spatial unit area and associated environmental features, allowing to leverage well-sampled regions to make predictions in environmentally similar but less-surveyed areas. By extrapolating rarefaction curves under asymptotic sampling effort, our approach yields estimates of total expected species richness for any spatial unit area, thereby recovering location-specific species-area relationships. Incorporating environmental context contributed to improve species richness estimates by 32% over the conventional Chao2 estimator. Shapley value analysis of the deep SAR model revealed insights into key drivers of biodiversity patterns. The analysis supported that environmental filtering is the primary driver of species richness patterns, with area *per se* effects and habitat diversity effects becoming increasingly important at larger spatial grains. Spatially explicit predictions of species richness and turnover uncovered scale-dependent biodiversity patterns, with mountainous regions exhibiting the highest species richness at coarse scales, despite showing relatively lower local richness at fine scales. These results collectively demonstrate that our approach effectively captures the multi-scale relationships between biodiversity drivers and species richness patterns.

The application of machine learning in macroecology research has predominantly focused on predicting species distributions (see, e.g., (Deneu et al., 2021; Brun et al., 2024; Gillespie et al., 2024)). However, many ecological and conservation questions require understanding macroecological properties at the community or ecosystem level. Our deep SAR model adopts a fundamentally different approach by directly modeling community-level biodiversity metrics rather than individual species distributions. By capturing how environmental conditions influence species richness across spatial scales without explicitly modeling individual species' ranges, our approach offers several advantages. First, it is more data-efficient as it leverages the aggregated signal from multiple species rather than requiring sufficient data for each species individually. Second, it can exploit general relationships between environmental conditions and species richness that remain consistent across biogeographic regions (Leroux et al., 2017; Dubuis et al., 2011). This enhances model transferability and generalization compared to species distribution models, which often suffer from limited occurrence data, particularly for rare species, and may not capture emergent community-level properties that arise from species interactions and assembly processes.

The theoretical functional form of the SAR has long been debated in ecology, with no consensus on the most appropriate model (Dengler, 2009). While the search for a theoretical functional forms is required in a low-data regime or for deriving general macroecological patterns, they are simplifications that cannot accommodate the complexity of realistic landscapes. Realistic landscapes are often heterogeneous, where species richness may rise idiosyncratically due to dispersal barriers, natural local variations, or anthropogenic stressors (Whittaker, 1972; Gering et al., 2003). Sampling theory allows us to leverage abundant ecological survey data for training deep neural networks, which have the capacity to capture these complex accumulation dynamics without imposing strong assumptions about the functional form.

Our deep SAR model provides a comprehensive framework for biodiversity assessment and conservation planning by enabling the estimation of environmental driver effects on species richness across spatial scales. For instance, our deep SAR model could enable habitat loss impact assessment by comparing predicted species richness between intact and degraded areas (Gotelli and Colwell, 2001; Matthews et al., 2021a; Thomas et al., 2004; Brooks et al., 2002), while capturing scale-dependent effects often overlooked in traditional assessments. Additionally, species turnover maps offer particularly valuable conservation insights. High-turnover regions indicate rapid species richness increase with area, suggesting that habitat loss may disproportionately impact regional biodiversity by eliminating unique assemblages (Socolar et al., 2016). Conversely, areas with high local richness but low turnover may exhibit greater resilience to localized habitat loss. Explainable artificial intelligence methods, such as Shapley values, enable us to quantify how environmental stressor effects on species richness vary across spatial scales, therefore allowing to enhance our understanding of biodiversity responses. Overall, our deep SAR model delivers critical information that can serve the multi-scale objectives of biodiversity conservation (Kunin et al., 2018).

From a machine learning perspective, predicting species richness from pools of ecological surveys represents a multiple instance learning (MIL) problem (Carbonneau et al., 2018). Ecological surveys correspond to instances, their aggregation generates training samples (bags), and predicting species richness involves predicting bag-level labels from instance-specific (sampling effort) and bag-specific (environmental covariates) features. With this perspective, modern MIL architectures using attention mechanisms could potentially improve species richness estimates (Ilse

et al., 2018). While we manually engineered environmental features by calculating means and standard deviations, convolutional neural networks or vision transformers could automatically extract higher-order statistics and leverage satellite imagery to characterize habitat fragmentation effects (Hanski et al., 2013; Rybicki and Hanski, 2013). Future improvements could leverage higher-resolution climate data to capture microenvironmental factors shaping local species assemblages (Dembicz et al., 2021), incorporate alternative biodiversity data sources such as citizen science species occurrence data (GBIF: The Global Biodiversity Information Facility, 2022), and extend predictions to other biodiversity metrics including Hill numbers that generalize species richness (Chao et al., 2014) or genetic diversity (De Kort et al., 2021). Enhanced uncertainty characterization beyond model ensembling represents another important direction for transparent biodiversity assessment.

## 4 Conclusion

Our study demonstrates how deep learning combined with sampling theory can effectively estimate scale-dependent macroecological properties from small-scale yet abundant ecological data. The deep SAR model provides a data-efficient approach to deliver comprehensive insights into biodiversity patterns, revealing the distinct effects of biodiversity drivers across scales. We anticipate future applications of our framework to capture complementary macroecological properties of ecosystems, such as functional or genetic diversity. This multi-scale prediction capacity is essential for attributing biodiversity changes to global change drivers and designing robust conservation strategies that account for the scale-dependency of ecological processes.

## 5 Methods

We aim to estimate *total species richness*  $S_T$ , the total number of species in a spatial unit  $A$  at a given location. However, biodiversity surveys typically sample only a small fraction of  $A$ , requiring extrapolation from these limited samples to estimate richness across the entire area. This extrapolation challenge has been addressed through various approaches (Elena Schmitz and Rahmann, 2025), but these methods typically focus on estimating total richness within a single spatial unit. Our approach introduces a key innovation by conditioning the extrapolation on features  $X$  associated with the spatial unit, including its area and statistics of environmental features within the spatial unit. This conditioning on  $X$  enables spatially explicit mapping of  $S_T = S_T(X)$  estimates across landscapes at multiple spatial scales.

Section 5.1 provides the required definitions and explains our methodological setup. Section 5.2 details the curve fitting procedure and neural network implementation. Section 5.3 describes the datasets used in our analysis.

### 5.1 Estimating total species richness from small samples

**Sampling process.** Let  $a_i$  be the union of a set of  $m = |i|$  small-scale samples  $a_{i_1}, \dots, a_{i_m}$  randomly placed in the spatial unit  $A$ :

$$a_i := a_{i_1} \cup \dots \cup a_{i_m} \subseteq A, \quad (1)$$

with corresponding locations  $x_{i_1}, \dots, x_{i_m}$  and pooled area  $|a_i|$ . We will denote such a set as a *sample set* and view a particular sample set as a realisation of a random variable. In the limit of infinite sample effort, we have

$$\lim_{m \rightarrow \infty} a_i = \lim_{m \rightarrow \infty} (a_{i_1} \cup \dots \cup a_{i_m}) = A. \quad (2)$$

In the sample set, we count species to obtain its *observed species richness*:

$$S(a_i) := \sum_{j=1}^{S_T} \mathbb{1}_{N_j(a_i) \geq 1}, \quad (3)$$

where  $\mathbb{1}_{(\cdot)}$  evaluates to 1 when the condition in its argument is true and to zero otherwise, and  $N_j(a_i)$  the number of individuals of species  $j$  in  $a_i$ . Randomly sampling over different  $i$  yields pairs  $|a_i| \mapsto S(a_i)$ . To avoid bias towards any particular  $i$ , we need a way to average over different realisations.

**Species rarefaction curve.** The curve that shows how *expected species richness* increases with sampling effort is known as a rarefaction curve. We can obtain it by taking an expectation conditional on sampling effort, where sampling effort may either be expressed in terms of sample size  $m = |\mathbf{i}|$  or in terms of pooled sample area  $|\mathbf{a}_i|$ . Because we will fit a species-area relation, we use the latter:

$$\mathcal{S}(a) := \mathbb{E} \left[ S(\mathbf{a}_i) \mid |\mathbf{a}_i| = a \right] = \sum_{j=1}^{S_T} \mathbb{P} \left[ N_j(\mathbf{a}_i) \geq 1 \mid |\mathbf{a}_i| = a \right], \quad (4)$$

where we used Eq. 3 and that the expectation of an indicator function is the probability of its argument. Defining

$$p_k(a) := \frac{1}{S_T} \sum_{j=1}^{S_T} \mathbb{P} \left[ N_j(\mathbf{a}_i) = k \mid |\mathbf{a}_i| = a \right], \quad (5)$$

the expected proportion of species in a sample with  $k$  individuals at effort  $a$ , we obtain

$$\mathcal{S}(a) = S_T \sum_{k=1}^{\infty} p_k(a) = S_T [1 - p_0(a)], \quad (6)$$

where we used that Eq. 5 sums to 1. As  $S_T$  denotes the number of species occurring in A,  $p_0(a)$  is the expected fraction of species occurring in A that are missed at effort  $a$ . We can write  $p_0$  and therefore  $\mathcal{S}(a)$  as (see SI Appendix S1.1; Harte et al. (2009))

$$p_0(a) = \sum_{n \geq 1} f_n^+ q_n(a), \quad \Rightarrow \quad \mathcal{S}(a) = S_T \left[ 1 - \sum_{n \geq 1} f_n^+ q_n(a) \right]. \quad (7)$$

where  $f_n^+$  is the zero-truncated species abundance distribution (SAD, over species present) in A and  $q_n(a)$  the probability of absence at effort  $a$  given  $n$  individuals in A.  $q_n$  depends only on how individuals are arranged within A. Thus the rarefaction curve depends jointly on the SAD, the spatial arrangement of individuals within A and the sampling process. By construction  $\mathcal{S}(0) = 0$  and  $\mathcal{S}(|A|) = S_T$ .

**Parametric estimation of the rarefaction curve.** We aim to estimate  $\mathcal{S}(a)$  by fitting functional forms to sampling data. In our choice of functional form, the case of uniform random placement (URP) is informative because it yields closed form solutions for the rarefaction curve in terms of  $a$ . Under URP, we have  $q_n(a) = (1 - a/|A|)^n$ , such that the rarefaction curve becomes (via Eq. 7; Coleman (1981); He and Legendre (2002)):

$$\mathcal{S}_u(\alpha; \vartheta) = S_T \left[ 1 - G\{f_{n,\vartheta}^+\}(1 - \alpha) \right], \quad (8)$$

where  $\alpha := a/|A|$  and  $G\{f_{n,\vartheta}^+\}$  the probability-generating function (PGF) of the SAD with parameters  $\vartheta$ . Table S1 shows examples for a selection of SADs under URP. For instance, when  $f_{n,\vartheta}^+$  is a geometric distribution with parameter  $\vartheta$ , then the rarefaction curve is the classic Michaelis–Menten type functional form  $\mathcal{S}_u(\alpha; \vartheta) = S_T \frac{\alpha}{\vartheta + (1-\vartheta)\alpha}$ . The URP case suggests that the functional form of the rarefaction equation can be obtained by first choosing the right parametric family of probability mass functions  $f_{n,\vartheta}^+$  with parameter(s)  $\vartheta$ , then obtaining the corresponding form of the rarefaction curve via Eq. 8, and finally obtaining the parameters  $\Theta = (S_T, \vartheta)$  by fitting it to data generated by the sampling process.

Real communities, however, exhibit spatial structure due to environmental heterogeneity and spatial interactions, so URP is typically violated. Moreover both spatial structure and the SAD generally differ between locations, so it would be highly restrictive to choose a single parametric family of probability mass functions. Hence, any chosen functional form  $g_\Theta(a)$  must be flexible enough as to fit diverse shapes regardless of the deviation from URP and differences between locations, but still satisfy monotonicity in  $a$  and reach  $S_T$  for large  $a$  ( $m \rightarrow \infty$ ). Parameters  $\Theta$  can be obtained by fitting  $g_\Theta$  to data pairs  $|\mathbf{a}_i| \mapsto S(\mathbf{a}_i)$ , generated through the sampling process described above, drawing  $\mathbf{a}_i$  randomly with replacement. Fitting can be performed using maximum likelihood estimation. Once  $g_\Theta$  is fitted, we can recover  $S_T$  as the limit of the rarefaction curve to large sampling effort.

**Four parameter Weibull function.** A flexible choice for the functional form  $g_{\Theta}$  is the four-parameter Weibull function (Zou et al., 2023):

$$g_{\Theta}(a) = c + (S_T - c)(1 - \exp[-(a/e)^b]), \quad (9)$$

which is at its minimum ( $c$ ) at  $a = 0$  and converges to its maximum ( $S_T$ ) as  $a$  becomes large. The offset  $c$  captures the species richness at the smallest scale at the grain of the data.  $b$  controls the shape parameter determining the rate of species accumulation, and  $e$  is the scale parameter representing the characteristic sampling effort. As visually depicted in Fig. 1b, we found that Eq. 9 provides a good fit for arbitrary SARs obtained through our method and with the data we used.

## 5.2 Deep SAR model

**Conditioning the rarefaction curve on environmental features and area of the spatial unit.** Rarefaction curves depend in general on the area and the environmental covariates associated with the spatial unit under consideration (Dengler and Oldeland, 2010). We make use of this dependence to map total species richness estimates over space. More precisely, to predict the observed species richness  $S$  of a spatial unit  $A$  with arbitrary size and location, we condition  $g_{\Theta}$  on features  $X$  associated with the spatial unit, which include its area and statistics of environmental features within the spatial unit. We use a neural network  $h_{\theta}$  to learn the mapping from the features  $X$  to the parameters  $\Theta$  of the rarefaction curve model  $g_{\Theta}$ :

$$\Theta = h_{\theta}(X) \quad (10)$$

The predicted expected species richness for a given sampling effort  $a$  is then

$$\mathbb{E}[S(a) | X] = g_{\Theta}(a, X) = g_{h_{\theta}(X)}(a). \quad (11)$$

The neural network  $h_{\theta}$  is trained by minimizing the loss function:

$$L(\theta) = \sum_{k=1}^K [g_{h_{\theta}(X_k)}(|a_{i_k}|) - S(a_{i_k})]^2, \quad a_{i_k} \subset A_k, \quad (12)$$

where  $S(a_{i_k})$  represents the observed species richness from  $m_k = |a_{i_k}|$  randomly selected surveys within spatial unit  $k$  with features  $X_k$ .

**Deep SAR model training.** We generated sample sets  $a_{i_k}$  by randomly placing spatial units  $A_k$  containing at least two ecological surveys, with log-transformed area  $\log |A_k|$  following a uniform distribution between  $10^4$  and  $10^{11}$  m<sup>2</sup>. Within each spatial unit  $A_k$ , we identified the  $M_k$  surveys from the EVA database whose coordinates fall within its bounds. We then selected a random subsample of  $m_k \leq M_k$  ecological surveys, where  $m_k$  follows a log-uniform discrete distribution  $m_k \sim \mathcal{U}_{\log}\{2, 3, \dots, M_k\}$  and calculated their observed species richness. We assessed how the number of training samples influences model performance and report the results in Fig. S1. Model performance increases with the number of sample sets, and we found that the optimal number is on the order of magnitude of the number of surveys used.

**Neural network architecture and hyperparameters.** Our deep SAR models employ fully connected multi-layer perceptrons implemented in PyTorch. The network architecture consists of 6 fully connected layers with 32, 128, 256, 256, 128, and 32 neurons respectively, using leaky ReLU activation functions. Input features include the spatial unit area and the mean and standard deviation of environmental variables within each spatial unit (detailed in Biodiversity data). For ensemble predictions used in Contribution of area and environment across spatial scales and Scale-specific patterns of plant species richness and turnover in Europe, we trained 5 independent models and aggregated their outputs using arithmetic mean. Standard deviations of ensemble predictions are provided in Fig. S6. We used batch sizes of 1024 samples over 100 epochs for training, which we found sufficient for convergence as shown in Fig. S5. We used the Adam optimizer (Kingma and Ba, 2014) with decoupled weight decay regularization (Loshchilov and Hutter, 2019) and a learning rate scheduler with 20-epoch patience and 0.5 decay factor. Data was split into 90% training and 10% validation subsets for both ablation studies and final ensemble models.

## 5.3 Data

**Biodiversity data.** We used a dataset of 502,724 vegetation plots from the European Vegetation Archive (Chytrý et al. (2016); <https://euroveg.org/eva-database/version/2023-02-04>; project 172; data retrieved on 27 February 2023). We selected only plots with available area information and coordinate uncertainty less than 1 km. We additionally discarded plots not located on land within Europe and excluded non-vascular taxa from the dataset. Vegetation plots were analyzed without distinction of habitat types. The data filtering resulted in 488,622 vegetation plots for downstream analyses (see Fig. S7). Additionally, we used the Global Inventory of Floristic Taxonomy (GIFT) database (Weigelt et al., 2020), filtered to select surveys occurring within continental Europe, resulting in 184 exhaustive species surveys. We harmonized species names between the EVA and GIFT databases following procedures detailed at <https://github.com/vboussange/DeepSAR>. This resulted in the EVA-based dataset comprising 9,480 distinct species, while the GIFT-based dataset comprised 33,729 distinct species.

**Environmental features.** We calculated environmental features using seven bioclimatic variables from the CHELSA dataset (Karger et al., 2021; Brun et al., 2022): mean annual air temperature (`bio1`), temperature seasonality (`bio4`), annual precipitation (`bio12`), precipitation seasonality (`bio15`), near-surface wind speed (`sfcWind`), potential evapotranspiration (`pet`), and surface downwelling shortwave radiation (`rsds`). These variables exhibit low pairwise correlations across the geographical extent (Spearman  $\rho < 0.5$ ). The associated mean climate features also show low correlations (Spearman  $\rho < 0.55$ ), whereas climate heterogeneity features display higher but still moderate correlations (Spearman  $\rho < 0.75$ ; see Fig. S3).

## 6 Data availability

The preprocessed EVA dataset with anonymized species names, the associated GIFT dataset anonymized with the same procedure, the pretrained weights of the deep SAR ensemble model, and tutorials for how to use it, are available under our GitHub repository at <https://github.com/vboussange/DeepSAR>. The original EVA dataset has restricted access and is available upon request at <https://euroveg.org/eva-database>. Climate data used in this study is available from the CHELSA database <https://chelsa-climate.org>. Scripts for downloading and processing the original GIFT database are included in our GitHub repository.

## 7 Code availability

The code used to train and evaluate the models and generate all figures is available under our GitHub repository at <https://github.com/vboussange/DeepSAR>.

## 8 Author contributions

V.B., B.W., P.B., J.T.M., G.M., J.P., T.S., N.E.Z., and D.N.K. conceived the study. V.B. developed the methodology and implemented the software. V.B. and B.W. performed the formal analysis. P.B., J.T.M., G.M., J.P., T.S., and D.N.K. contributed to methodological development. Data were provided by I.A., H.B., M.C., S.K., Z.L., M.V., I.B., K.T.E., J.L., and J.-C.S. V.B. wrote the original draft. All authors contributed to manuscript review and editing. N.E.Z. and D.N.K. acquired funding. D.N.K. supervised the project. Authors are listed alphabetically in the following order: the core team leading the study (V.B., P.B., J.T.M., G.M., J.P., T.S., N.E.Z.), followed by contributors from the FeedBaCks consortium (I.A., H.B., M.C., S.K., Z.L., M.V.) and EVA data custodians (I.B., K.T.E., J.L., J.-C.S.), also alphabetically within each group, and last the senior author (D.N.K.).

## 9 Acknowledgements

This research was funded through the 2019-2020 BiodivERsA joint call for research proposals, under the BiodivClim ERA-Net COFUND program, and with the funding organisations Swiss National Science Foundation SNF (project:

FeedBaCks, 193907), the German Research Foundation (DFG BR 1698/21-1, DFG HI 1538/16-1), and the Technology Agency of the Czech Republic (SS70010002). N.E.Z. considers this work a contribution to the SPEED2ZERO Joint Initiative, which received support from the ETH-Board under the Joint Initiatives scheme. J.C.S. considers this work a contribution to Center for Ecological Dynamics in a Novel Biosphere (ECONOVO), funded by Danish National Research Foundation (grant DNRF173).

## References

- IPBES. Global assessment report on biodiversity and ecosystem services of the Intergovernmental Science-Policy Platform on Biodiversity and Ecosystem Services. Technical report, Zenodo, May 2019. URL <https://zenodo.org/records/6417333>.
- Simon M Smart, Ken Thompson, Robert H Marrs, Mike G Le Duc, Lindsay C Maskell, and Leslie G Firbank. Biotic homogenization and changes in species diversity across human-modified ecosystems. *Proceedings of the Royal Society B: Biological Sciences*, 273(1601):2659–2665, October 2006. ISSN 0962-8452, 1471-2954. doi: 10.1098/rspb.2006.3630.
- Lenore Fahrig. Relative Effects of Habitat Loss and Fragmentation on Population Extinction. *The Journal of Wildlife Management*, 61(3):603–610, 1997. ISSN 0022-541X. doi: 10.2307/3802168.
- Sean L. Maxwell, Richard A. Fuller, Thomas M. Brooks, and James E. M. Watson. Biodiversity: The ravages of guns, nets and bulldozers. *Nature*, 536(7615):143–145, August 2016. ISSN 1476-4687. doi: 10.1038/536143a.
- Rohan D. Simkin, Karen C. Seto, Robert I. McDonald, and Walter Jetz. Biodiversity impacts and conservation implications of urban land expansion projected to 2050. *Proceedings of the National Academy of Sciences*, 119(12):e2117297119, March 2022. doi: 10.1073/pnas.2117297119.
- Petr Keil, David Storch, and Walter Jetz. On the decline of biodiversity due to area loss. *Nature Communications*, 6(1):8837, November 2015. ISSN 2041-1723. doi: 10.1038/ncomms9837.
- Ryan P. Powers and Walter Jetz. Global habitat loss and extinction risk of terrestrial vertebrates under future land-use-change scenarios. *Nature Climate Change*, 9(4):323–329, April 2019. ISSN 1758-6798. doi: 10.1038/s41558-019-0406-z.
- Tim Newbold. Future effects of climate and land-use change on terrestrial vertebrate community diversity under different scenarios. *Proceedings of the Royal Society B: Biological Sciences*, 285(1881):20180792, June 2018. ISSN 0962-8452, 1471-2954. doi: 10.1098/rspb.2018.0792.
- Fangliang He and Stephen P. Hubbell. Species–area relationships always overestimate extinction rates from habitat loss. *Nature*, 473(7347):368–371, May 2011. ISSN 1476-4687. doi: 10.1038/nature09985.
- Carsten Rahbek. The role of spatial scale and the perception of large-scale species-richness patterns. *Ecology Letters*, 8(2):224–239, 2005. ISSN 1461-0248. doi: 10.1111/j.1461-0248.2004.00701.x.
- IPBES, M. Rounsevell, M. Fischer, A. T. M. Rando, and A. Mader. The IPBES regional assessment report on biodiversity and ecosystem services for Europe and Central Asia. Technical report, Zenodo, March 2018.
- Robert V O'Neill. *A hierarchical concept of ecosystems*. Number 23. Princeton University Press, 1986.
- Olof Arrhenius. Species and Area. *Journal of Ecology*, 9(1):95–99, 1921. ISSN 0022-0477. doi: 10.2307/2255763.
- Thomas J. Matthews, Kostas A. Triantis, and Robert J. Whittaker, editors. *The Species–Area Relationship: Theory and Application*. Ecology, Biodiversity and Conservation. Cambridge University Press, Cambridge, 2021a. ISBN 978-1-108-47707-9. doi: 10.1017/9781108569422.
- John M. Halley, Vasiliki Sgardeli, and Nikolaos Monokrousos. Species–area relationships and extinction forecasts. *Annals of the New York Academy of Sciences*, 1286(1):50–61, 2013. ISSN 1749-6632. doi: 10.1111/nyas.12073.

- Robert J Whittaker and José María Fernández-Palacios. *Island Biogeography: Ecology, Evolution, and Conservation*. Oxford University Press, 2007.
- Kostas A. Triantis, François Guilhaumon, and Robert J. Whittaker. The island species–area relationship: Biology and statistics. *Journal of Biogeography*, 39(2):215–231, 2012. ISSN 1365-2699. doi: 10.1111/j.1365-2699.2011.02652.x.
- Hanna Tuomisto. A diversity of beta diversities: Straightening up a concept gone awry. Part 1. Defining beta diversity as a function of alpha and gamma diversity. *Ecography*, 33(1):2–22, February 2010. ISSN 09067590. doi: 10.1111/j.1600-0587.2009.05880.x.
- Jürgen Dengler. Which function describes the species-area relationship best? A review and empirical evaluation. *Journal of Biogeography*, 36(4):728–744, April 2009. ISSN 03050270, 13652699. doi: 10.1111/j.1365-2699.2008.02038.x.
- François Guilhaumon, Olivier Gimenez, Kevin J. Gaston, and David Mouillot. Taxonomic and regional uncertainty in species-area relationships and the identification of richness hotspots. *Proceedings of the National Academy of Sciences*, 105(40):15458–15463, October 2008. doi: 10.1073/pnas.0803610105.
- E. F. Connor and E. D. McCoy. Species–Area Relationships. In Simon A Levin, editor, *Encyclopedia of Biodiversity (Second Edition)*, pages 640–650. Academic Press, Waltham, January 2013. ISBN 978-0-12-384720-1. doi: 10.1016/B978-0-12-384719-5.00132-5.
- Ryan A. Chisholm, Nicholas Z. W. Fong, Daniel A. Friess, and Andre S. Rovai. Inferring community assembly processes from mangrove species–area relationships. *Oikos*, 2025(7), July 2025. ISSN 0030-1299, 1600-0706. doi: 10.1002/oik.11095.
- Luís Borda-de-Água, M. Manuela Neves, Luise Quoss, Stephen P. Hubbell, Filipe S. Dias, and Henrique M. Pereira. Modelling the species-area relationship using extreme value theory. *Nature Communications*, 16(1):4045, April 2025. ISSN 2041-1723. doi: 10.1038/s41467-025-59239-7.
- Matthew G. Betts, Lenore Fahrig, Adam S. Hadley, Katherine E. Halstead, Jeff Bowman, W. Douglas Robinson, John A. Wiens, and David B. Lindenmayer. A species-centered approach for uncovering generalities in organism responses to habitat loss and fragmentation. *Ecography*, 37(6):517–527, June 2014. ISSN 0906-7590, 1600-0587. doi: 10.1111/ecog.00740.
- Thomas J. Matthews, François Guilhaumon, Kostas A. Triantis, Michael K. Borregaard, and Robert J. Whittaker. On the form of species–area relationships in habitat islands and true islands. *Global Ecology and Biogeography*, 25(7):847–858, 2016. ISSN 1466-8238. doi: 10.1111/geb.12269.
- Fangliang He and Pierre Legendre. Species Diversity Patterns Derived from Species–Area Models. *Ecology*, 83(5): 1185–1198, 2002. ISSN 1939-9170. doi: 10.1890/0012-9658(2002)083[1185:SDPDFS]2.0.CO;2.
- Patrick Weigelt and Holger Kreft. Quantifying island isolation – insights from global patterns of insular plant species richness. *Ecography*, 36(4):417–429, 2013. ISSN 1600-0587. doi: 10.1111/j.1600-0587.2012.07669.x.
- Thomas J. Matthews, François Rigal, Konstantinos Proios, Kostas A. Triantis, and Robert J. Whittaker. Explaining Variation in Island Species–Area Relationship (ISAR) Model Parameters between Different Archipelago Types: Expanding a Global Model of ISARs. In Thomas J. Matthews, Kostas A. Triantis, and Robert J. Whittaker, editors, *The Species–Area Relationship*, pages 51–77. Cambridge University Press, 1 edition, March 2021b. ISBN 978-1-108-56942-2 978-1-108-47707-9 978-1-108-70187-7. doi: 10.1017/9781108569422.007.
- Werner Ulrich, Thomas J. Matthews, Idoia Biurrun, Juan Antonio Campos, Patryk Czortek, Iwona Dembicz, Franz Essl, Goffredo Filibeck, Gian-Pietro Giusso del Galdo, Behlül Güler, Alireza Naqinezhad, Péter Török, and Jürgen Dengler. Environmental drivers and spatial scaling of species abundance distributions in Palaeartic grassland vegetation. *Ecology*, 103(8):e3725, 2022. ISSN 1939-9170. doi: 10.1002/ecy.3725.

- Stina Drakare, Jack J. Lennon, and Helmut Hillebrand. The imprint of the geographical, evolutionary and ecological context on species–area relationships. *Ecology Letters*, 9(2):215–227, 2006. ISSN 1461-0248. doi: 10.1111/j.1461-0248.2005.00848.x.
- Katherine J. Willis and Robert J. Whittaker. Species Diversity–Scale Matters. *Science*, 295(5558):1245–1248, February 2002. doi: 10.1126/science.1067335.
- Will R. Turner and Even Tjørve. Scale-dependence in species-area relationships. *Ecography*, 28(6):721–730, 2005. ISSN 1600-0587. doi: 10.1111/j.2005.0906-7590.04273.x.
- J. A. Wiens. Spatial Scaling in Ecology. *Functional Ecology*, 3(4):385, 1989. ISSN 02698463. doi: 10.2307/2389612.
- K. A. Triantis, M. Mylonas, K. Lika, and K. Vardinoyannis. A model for the species–area–habitat relationship. *Journal of Biogeography*, 30(1):19–27, 2003. ISSN 1365-2699. doi: 10.1046/j.1365-2699.2003.00805.x.
- Athanasios S. Kallimanis, Antonis D. Mazaris, Joseph Tzanopoulos, John M. Halley, John D. Pantis, and Stefanos P. Sgardelis. How does habitat diversity affect the species–area relationship? *Global Ecology and Biogeography*, 17(4):532–538, 2008. ISSN 1466-8238. doi: 10.1111/j.1466-8238.2008.00393.x.
- Attila Kalmar and David J. Currie. A Unified Model of Avian Species Richness on Islands and Continents. *Ecology*, 88(5):1309–1321, 2007. ISSN 1939-9170. doi: 10.1890/06-1368.
- William E. Kunin, John Harte, Fangliang He, Cang Hui, R. Todd Jobe, Annette Ostling, Chiara Polce, Arnošt Šizling, Adam B. Smith, Krister Smith, Simon M. Smart, David Storch, Even Tjørve, Karl-Inne Ugland, Werner Ulrich, and Varun Varma. Upscaling biodiversity: Estimating the species–area relationship from small samples. *Ecological Monographs*, 88(2):170–187, May 2018. ISSN 0012-9615, 1557-7015. doi: 10.1002/ecm.1284.
- Jeanne Portier, Florian Zellweger, Jürgen Zell, Iciar Alberdi Asensio, Michal Bosela, Johannes Breidenbach, Vladimír Šebeň, Rafael O. Wüest, and Brigitte Rohner. Plot size matters: Toward comparable species richness estimates across plot-based inventories. *Ecology and Evolution*, 12(6), June 2022. ISSN 2045-7758, 2045-7758. doi: 10.1002/ece3.8965.
- Anne Chao, Nicholas J. Gotelli, T. C. Hsieh, Elizabeth L. Sander, K. H. Ma, Robert K. Colwell, and Aaron M. Ellison. Rarefaction and extrapolation with Hill numbers: A framework for sampling and estimation in species diversity studies. *Ecological Monographs*, 84(1):45–67, 2014. ISSN 1557-7015. doi: 10.1890/13-0133.1.
- Johanna Elena Schmitz and Sven Rahmann. A comprehensive review and evaluation of species richness estimation. *Briefings in Bioinformatics*, 26(2):bbaf158, March 2025. ISSN 1467-5463, 1477-4054. doi: 10.1093/bib/bbaf158.
- Jorge Soberón M. and Jorge Llorente B. The Use of Species Accumulation Functions for the Prediction of Species Richness. *Conservation Biology*, 7(3):480–488, 1993. ISSN 1523-1739. doi: 10.1046/j.1523-1739.1993.07030480.x.
- Nicholas J. Gotelli and Robert K. Colwell. Quantifying biodiversity: Procedures and pitfalls in the measurement and comparison of species richness. *Ecology Letters*, 4(4):379–391, 2001. ISSN 1461-0248. doi: 10.1046/j.1461-0248.2001.00230.x.
- Milan Chytrý, Stephan M. Hennekens, Borja Jiménez-Alfaro, Ilona Knollová, Jürgen Dengler, Florian Jansen, Flavia Landucci, Joop H.J. Schaminée, Svetlana Ačić, Emiliano Agrillo, Didem Ambarlı, Pierangela Angelini, Iva Apostolova, Fabio Attorre, Christian Berg, Erwin Bergmeier, Idoia Biurrun, Zoltán Botta-Dukát, Henry Brisse, Juan Antonio Campos, Luis Carlón, Andraž Čarni, Laura Casella, János Csiky, Renata Čušterevska, Zora Dajić Stevanović, Jiří Danihelka, Els De Bie, Patrice de Ruffray, Michele De Sanctis, W. Bernhard Dickoré, Panayotis Dimopoulos, Dmytro Dubyna, Tetiana Dziuba, Rasmus Ejrnæs, Nikolai Ermakov, Jörg Ewald, Giuliano Fanelli, Federico Fernández-González, Úna FitzPatrick, Xavier Font, Itziar García-Mijangos, Rosario G. Gavilán, Valentin Golub, Riccardo Guarino, Rense Haveman, Adrian Indreica, Deniz Işık Gürsoy, Ute Jandt, John A.M. Janssen, Martin Jiroušek, Zygmunt Kącki, Ali Kavgacı, Martin Kleikamp, Vitaliy Kolomyichuk, Mirjana Krstivojević Čuk, Daniel Krstonošić, Anna Kuzemko, Jonathan Lenoir, Tatiana Lysenko, Corrado Marcenò, Vassilij Martynenko, Dana

- Michalcová, Jesper Erenskjold Moeslund, Viktor Onyshchenko, Hristo Pedashenko, Aaron Pérez-Haase, Tomáš Peterka, Vadim Prokhorov, Valerijus Rašomavičius, Maria Pilar Rodríguez-Rojo, John S. Rodwell, Tatiana Rogova, Eszter Ruprecht, Solvita Rūsiņa, Gunnar Seidler, Jozef Šibík, Urban Šilc, Željko Škvorc, Desislava Sopotlieva, Zvezdana Stančić, Jens-Christian Svenning, Grzegorz Swacha, Ioannis Tsiripidis, Pavel Dan Turtureanu, Emin Uğurlu, Domas Uogintas, Milan Valachovič, Yulia Vashenyak, Kiril Vassilev, Roberto Venanzoni, Risto Virtanen, Lynda Weekes, Wolfgang Willner, Thomas Wohlgemuth, and Sergey Yamalov. European Vegetation Archive (EVA): An integrated database of European vegetation plots. *Applied Vegetation Science*, 19(1):173–180, 2016. ISSN 1654-109X. doi: 10.1111/avsc.12191.
- Patrick Weigelt, Christian König, and Holger Kreft. GIFT – A Global Inventory of Floras and Traits for macroecology and biogeography. *Journal of Biogeography*, 47(1):16–43, 2020. ISSN 1365-2699. doi: 10.1111/jbi.13623.
- Edward F. Connor and Earl D. McCoy. The Statistics and Biology of the Species-Area Relationship. *The American Naturalist*, 113(6):791–833, June 1979. ISSN 0003-0147, 1537-5323. doi: 10.1086/283438.
- Scott M Lundberg and Su-In Lee. A unified approach to interpreting model predictions. In I. Guyon, U. Von Luxburg, S. Bengio, H. Wallach, R. Fergus, S. Vishwanathan, and R. Garnett, editors, *Advances in Neural Information Processing Systems*, volume 30. Curran Associates, Inc., 2017.
- R H Whittaker. EVOLUTION AND MEASUREMENT OF SPECIES DIVERSITY. *TAXON*, 21(2-3):213–251, May 1972. ISSN 0040-0262. doi: 10.2307/1218190.
- Mark Vellend. Conceptual Synthesis in Community Ecology. *The Quarterly Review of Biology*, 85(2):183–206, June 2010. ISSN 0033-5770. doi: 10.1086/652373.
- Anke Stein, Katharina Gerstner, and Holger Kreft. Environmental heterogeneity as a universal driver of species richness across taxa, biomes and spatial scales. *Ecology Letters*, 17(7):866–880, 2014. ISSN 14610248. doi: 10.1111/ele.12277.
- Hong Qian and Robert E. Ricklefs. Disentangling the effects of geographic distance and environmental dissimilarity on global patterns of species turnover. *Global Ecology and Biogeography*, 21(3):341–351, 2012. ISSN 1466-8238. doi: 10.1111/j.1466-8238.2011.00672.x.
- Richard Field, Bradford A. Hawkins, Howard V. Cornell, David J. Currie, J. Alexandre F. Diniz-Filho, Jean-François Guégan, Dawn M. Kaufman, Jeremy T. Kerr, Gary G. Mittelbach, Thierry Oberdorff, Eileen M. O'Brien, and John R. G. Turner. Spatial species-richness gradients across scales: A meta-analysis. *Journal of Biogeography*, 36(1):132–147, 2009. ISSN 1365-2699. doi: 10.1111/j.1365-2699.2008.01963.x.
- Lirong Cai, Holger Kreft, Amanda Taylor, Pierre Denelle, Julian Schrader, Franz Essl, Mark Van Kleunen, Jan Pergl, Petr Pyšek, Anke Stein, Marten Winter, Julie F. Barcelona, Nicol Fuentes, Inderjit, Dirk Nikolaus Karger, John Kartesz, Andreij Kuprijanov, Misako Nishino, Daniel Nickrent, Arkadiusz Nowak, Annette Patzelt, Pieter B. Pelser, Paramjit Singh, Jan J. Wieringa, and Patrick Weigelt. Global models and predictions of plant diversity based on advanced machine learning techniques. *New Phytologist*, 237(4):1432–1445, February 2023. ISSN 0028-646X, 1469-8137. doi: 10.1111/nph.18533.
- Alexandre Antonelli, W. Daniel Kissling, Suzette G.A. Flantua, Mauricio A. Bermúdez, Andreas Mulch, Alexandra N. Muellner-Riehl, Holger Kreft, H. Peter Linder, Catherine Badgley, Jon Fjeldså, Susanne A. Fritz, Carsten Rahbek, Frédéric Herman, Henry Hooghiemstra, and Carina Hoorn. Geological and climatic influences on mountain biodiversity. *Nature Geoscience*, 11(10):718–725, 2018. ISSN 17520908. doi: 10.1038/s41561-018-0236-z.
- Benjamin Deneu, Maximilien Servajean, Pierre Bonnet, Christophe Botella, François Munoz, and Alexis Joly. Convolutional neural networks improve species distribution modelling by capturing the spatial structure of the environment. *PLOS Computational Biology*, 17(4):e1008856, April 2021. ISSN 1553-7358. doi: 10.1371/journal.pcbi.1008856.

- Philipp Brun, Dirk N. Karger, Damaris Zurell, Patrice Descombes, Lucienne C. de Witte, Riccardo de Lutio, Jan Dirk Wegner, and Niklaus E. Zimmermann. Multispecies deep learning using citizen science data produces more informative plant community models. *Nature Communications*, 15(1):4421, May 2024. ISSN 2041-1723. doi: 10.1038/s41467-024-48559-9.
- Lauren E. Gillespie, Megan Ruffley, and Moises Exposito-Alonso. Deep learning models map rapid plant species changes from citizen science and remote sensing data. *Proceedings of the National Academy of Sciences*, 121(37): e2318296121, September 2024. doi: 10.1073/pnas.2318296121.
- Shawn J. Leroux, Cécile H. Albert, Anne-Sophie Lafuite, Bronwyn Rayfield, Shaopeng Wang, and Dominique Gravel. Structural uncertainty in models projecting the consequences of habitat loss and fragmentation on biodiversity. *Ecography*, 40(1):36–47, 2017. ISSN 1600-0587. doi: 10.1111/ecog.02542.
- Anne Dubuis, Julien Pottier, Vanessa Rion, Loïc Pellissier, Jean-Paul Theurillat, and Antoine Guisan. Predicting spatial patterns of plant species richness: A comparison of direct macroecological and species stacking modelling approaches. *Diversity and Distributions*, 17(6):1122–1131, 2011. ISSN 1472-4642. doi: 10.1111/j.1472-4642.2011.00792.x.
- Jon C. Gering, Thomas O. Crist, and Joseph A. Veech. Additive Partitioning of Species Diversity across Multiple Spatial Scales: Implications for Regional Conservation of Biodiversity. *Conservation Biology*, 17(2):488–499, 2003. ISSN 1523-1739. doi: 10.1046/j.1523-1739.2003.01465.x.
- Chris D. Thomas, Alison Cameron, Rhys E. Green, Michel Bakkenes, Linda J. Beaumont, Yvonne C. Collingham, Barend F. N. Erasmus, Marinez Ferreira de Siqueira, Alan Grainger, Lee Hannah, Lesley Hughes, Brian Huntley, Albert S. van Jaarsveld, Guy F. Midgley, Lera Miles, Miguel A. Ortega-Huerta, A. Townsend Peterson, Oliver L. Phillips, and Stephen E. Williams. Extinction risk from climate change. *Nature*, 427(6970):145–148, January 2004. ISSN 1476-4687. doi: 10.1038/nature02121.
- Thomas M. Brooks, Russell A. Mittermeier, Cristina G. Mittermeier, Gustavo A. B. Da Fonseca, Anthony B. Rylands, William R. Konstant, Penny Flick, John Pilgrim, Sara Oldfield, Georgina Magin, and Craig Hilton-Taylor. Habitat Loss and Extinction in the Hotspots of Biodiversity. *Conservation Biology*, 16(4):909–923, 2002. ISSN 1523-1739. doi: 10.1046/j.1523-1739.2002.00530.x.
- Jacob B. Socolar, James J. Gilroy, William E. Kunin, and David P. Edwards. How Should Beta-Diversity Inform Biodiversity Conservation? *Trends in Ecology & Evolution*, 31(1):67–80, January 2016. ISSN 0169-5347. doi: 10.1016/j.tree.2015.11.005.
- Marc-André Carbonneau, Veronika Cheplygina, Eric Granger, and Ghyslain Gagnon. Multiple instance learning: A survey of problem characteristics and applications. *Pattern Recognition*, 77:329–353, May 2018. ISSN 00313203. doi: 10.1016/j.patcog.2017.10.009.
- Maximilian Ilse, Jakub M. Tomczak, and Max Welling. Attention-based Deep Multiple Instance Learning, June 2018.
- Ilkka Hanski, Gustavo A. Zurita, M. Isabel Bellocq, and Joel Rybicki. Species–fragmented area relationship. *Proceedings of the National Academy of Sciences*, 110(31):12715–12720, July 2013. doi: 10.1073/pnas.1311491110.
- Joel Rybicki and Ilkka Hanski. Species–area relationships and extinctions caused by habitat loss and fragmentation. *Ecology Letters*, 16(s1):27–38, 2013. ISSN 1461-0248. doi: 10.1111/ele.12065.
- Iwona Dembicz, Jürgen Dengler, Manuel J. Steinbauer, Thomas J. Matthews, Sándor Bartha, Sabina Burrascano, Alessandro Chiarucci, Goffredo Filibeck, François Gillet, Monika Janišová, Salza Palpurina, David Storch, Werner Ulrich, Svetlana Ačić, Steffen Boch, Juan Antonio Campos, Laura Cancellieri, Marta Carboni, Giampiero Ciaschetti, Timo Conradi, Pieter De Frenne, Jiri Dolezal, Christian Dolnik, Franz Essl, Edy Fantinato, Itziar García-Mijangos, Gian Pietro Giusso del Galdo, John-Arvid Grytnes, Riccardo Guarino, Behlül Güler, Jutta Kapfer, Ewelina Klichowska, Łukasz Kozub, Anna Kuzemko, Swantje Löbel, Michael Manthey, Corrado Marcenò, Anne Mimet, Alireza Naqinezhad, Jalil Noroozi, Arkadiusz Nowak, Harald Pauli, Robert K. Peet, Vincent Pellissier, Remigiusz Pielech,

Massimo Terzi, Emin Uğurlu, Orsolya Valkó, Iuliia Vasheniak, Kiril Vassilev, Denys Vynokurov, Hannah J. White, Wolfgang Willner, Manuela Winkler, Sebastian Wolfrum, Jinghui Zhang, and Idoia Biurrun. Fine-grain beta diversity of Palaearctic grassland vegetation. *Journal of Vegetation Science*, 32(3):e13045, 2021. ISSN 1654-1103. doi: 10.1111/jvs.13045.

GBIF: The Global Biodiversity Information Facility. What is GBIF? 2022.

H. De Kort, J. G. Prunier, S. Ducatez, O. Honnay, M. Baguette, V. M. Stevens, and S. Blanchet. Life history, climate and biogeography interactively affect worldwide genetic diversity of plant and animal populations. *Nature Communications*, 12(1):516, January 2021. ISSN 2041-1723. doi: 10.1038/s41467-021-20958-2.

John Harte, Adam B Smith, and David Storch. Biodiversity scales from plots to biomes with a universal species–area curve. *Ecology letters*, 12(8):789–797, 2009.

Bernard D. Coleman. On random placement and species-area relations. *Mathematical Biosciences*, 54(3):191–215, 1981. ISSN 0025-5564. doi: [https://doi.org/10.1016/0025-5564\(81\)90086-9](https://doi.org/10.1016/0025-5564(81)90086-9). URL <https://www.sciencedirect.com/science/article/pii/0025556481900869>.

Yi Zou, Peng Zhao, and Jan Christoph Axmacher. Estimating total species richness: Fitting rarefaction by asymptotic approximation. *Ecosphere*, 14(1):e4363, January 2023. ISSN 2150-8925, 2150-8925. doi: 10.1002/ecs2.4363.

Jürgen Dengler and Jens Oldeland. Effects of sampling protocol on the shapes of species richness curves. *Journal of Biogeography*, 37(9):1698–1705, September 2010. ISSN 0305-0270, 1365-2699. doi: 10.1111/j.1365-2699.2010.02322.x.

Diederik P. Kingma and Jimmy Ba. Adam: A Method for Stochastic Optimization. pages 1–15, December 2014.

Ilya Loshchilov and Frank Hutter. Decoupled Weight Decay Regularization, January 2019.

Dirk Nikolaus Karger, Olaf Conrad, Jürgen Böhrer, Tobias Kawohl, Holger Kreft, Rodrigo Wilber Soria-Auza, Niklaus E. Zimmermann, H. Peter Linder, and Michael Kessler. Climatologies at high resolution for the earth's land surface areas, 2021.

Philipp Brun, Niklaus E. Zimmermann, Chantal Hari, Loïc Pellissier, and Dirk Nikolaus Karger. Global climate-related predictors at kilometer resolution for the past and future. *Earth System Science Data*, 14(12):5573–5603, December 2022. ISSN 1866-3508. doi: 10.5194/essd-14-5573-2022.

## S1 Supplementary text

### S1.1 Decomposition of $p_0$

**Step 1. Definition.**

$$p_0(a) := \mathbb{P}(N(a) = 0 \mid N(\mathbf{A}) \geq 1). \quad (\text{S1})$$

**Step 2. Law of total probability for conditional probabilities.**

$$\mathbb{P}(N(a) = 0 \mid N(\mathbf{A}) \geq 1) = \sum_{n \geq 1} \mathbb{P}(N(a) = 0 \mid N(\mathbf{A}) = n) \mathbb{P}(N(\mathbf{A}) = n \mid N(\mathbf{A}) \geq 1). \quad (\text{S2})$$

**Step 3. Identify ZT-SAD and spatial factor.**

$$f_n^+ := \mathbb{P}(N(\mathbf{A}) = n \mid N(\mathbf{A}) \geq 1), \quad q_n(a) := \mathbb{P}(N(a) = 0 \mid N(\mathbf{A}) = n), \quad (\text{S3})$$

so

$$p_0(a) = \sum_{n \geq 1} f_n^+ q_n(a). \quad (\text{S4})$$

**Step 4. Special case: uniform random placement.** If  $q_n(a) = (1 - \alpha)^n$  with  $\alpha = a/|\mathbf{A}|$  and  $G\{f_n^+\}(z) = \sum_{n \geq 1} f_n^+ z^n$ , then

$$p_0(a) = G\{f_n^+\}(1 - \alpha), \quad (\text{S5})$$

which matches the result of Coleman (1981).

## S2 Supplementary table

SAD (ZT)	$f_n^+$ (PMF over species)	$G\{f_n^+\}(z)$ (PGF of SAD)	$\mathcal{S}(\alpha)$	Refs
Logseries( $x$ )	$f_n^+ = \frac{x^n}{n[-\ln(1-x)]}, n \geq 1$	$G\{f_n^+\}(z) = \frac{\ln(1-xz)}{\ln(1-x)}$	$\mathcal{S}(\alpha) = S_T \left[1 - \frac{\ln(1-x(1-\alpha))}{\ln(1-x)}\right]$	Coleman (1981); He and Legendre (2002)
Pois $^+(\mu)$	$f_n^+ = \frac{e^{-\mu} \mu^n / n!}{1 - e^{-\mu}}, n \geq 1$	$G\{f_n^+\}(z) = \frac{e^{\mu(z-1)} - e^{-\mu}}{1 - e^{-\mu}}$	$\mathcal{S}(\alpha) = S_T \frac{1 - e^{-\mu\alpha}}{1 - e^{-\mu}}$	–
NB $^+(r, p)$	$f_n^+ = \frac{\binom{n+r-1}{n} (1-p)^n p^r}{1 - p^r}, n \geq 1$	$G\{f_n^+\}(z) = \frac{\left(\frac{p}{1 - (1-p)z}\right)^r - p^r}{1 - p^r}$	$\mathcal{S}(\alpha) = S_T \frac{1 - \left(\frac{p}{p + (1-p)\alpha}\right)^r}{1 - p^r}$	He and Legendre (2002)
Geom $^+(p)^*$	$f_n^+ = p(1-p)^{n-1}, n \geq 1$	$G\{f_n^+\}(z) = \frac{pz}{1 - (1-p)z}$	$\mathcal{S}(\alpha) = S_T \frac{\alpha}{p + (1-p)\alpha}$	He and Legendre (2002)
Most even	$f_{n^*}^+ = 1$ with $n^* = N/S_T \in \mathbb{N}$ ; rest 0	$G\{f_n^+\}(z) = z^{N/S_T}$	$\mathcal{S}(\alpha) = S_T [1 - (1-\alpha)^{N/S_T}]$	He and Legendre (2002)
Most uneven	$f_1^+ = \frac{S_T - 1}{S_T}, f_{N-S_T+1}^+ = \frac{1}{S_T}$ ; rest 0	$G\{f_n^+\}(z) = \frac{S_T - 1}{S_T} z + \frac{1}{S_T} z^{N-S_T+1}$	$\mathcal{S}(\alpha) = 1 + (S_T - 1)\alpha - (1-\alpha)^{N-S_T+1}$	He and Legendre (2002)

Table S1: Expected species richness for uniform random placement for a selection of SADs, with the event of an individual falling into  $a$  being a Bernoulli trial with probability parameter  $\alpha := a/|A|$ . All formulas use  $\mathcal{S}(\alpha) = \mathbb{E}[S(\alpha)] = S_T [1 - G\{f_n^+\}(1-\alpha)]$ . SAD = species abundance distribution; ZT = zero-truncated. \*Note that Geom $^+(p) = \text{NB}^+(1, p)$ .

### S3 Supplementary figures

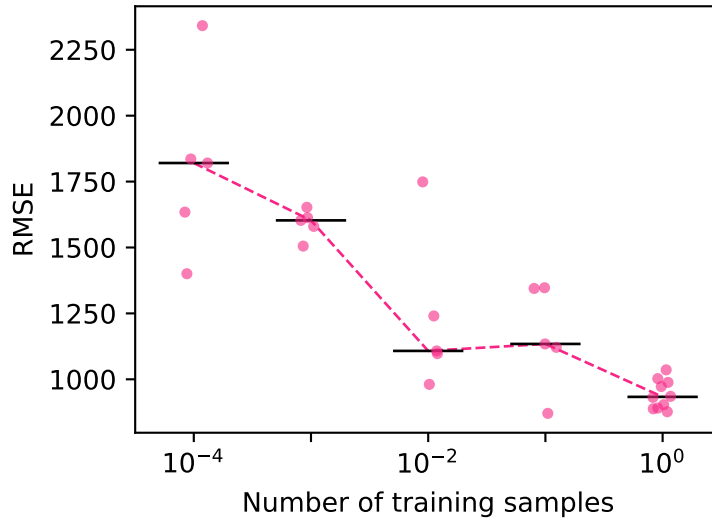


Figure S1: **Model's performance in predicting the EVA-based test dataset against the proportion of generated training samples relative to the number of surveys.** These results demonstrate that the optimal number of training data samples, generated through random pooling of vegetation plots, is on the order of magnitude of the number of surveys.

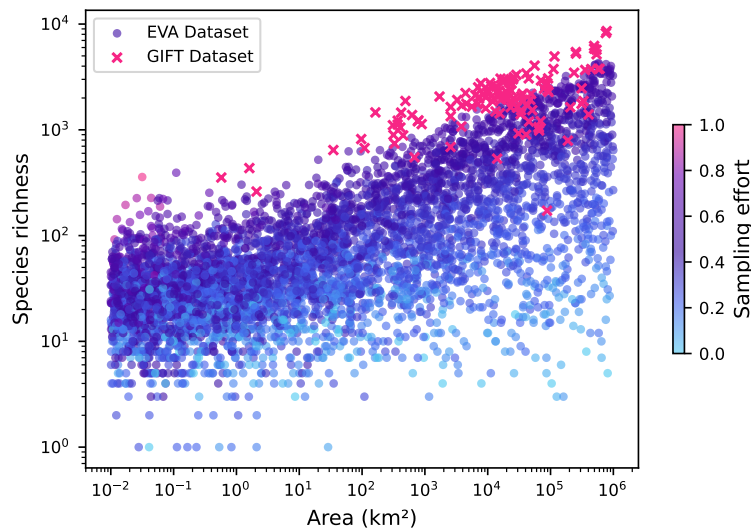


Figure S2: **Species richness against habitat area and sampling effort, for the EVA-based and GIFT-based datasets.** The sampling effort is calculated as the ratio of the logarithm of observed area over the logarithm of the habitat area.

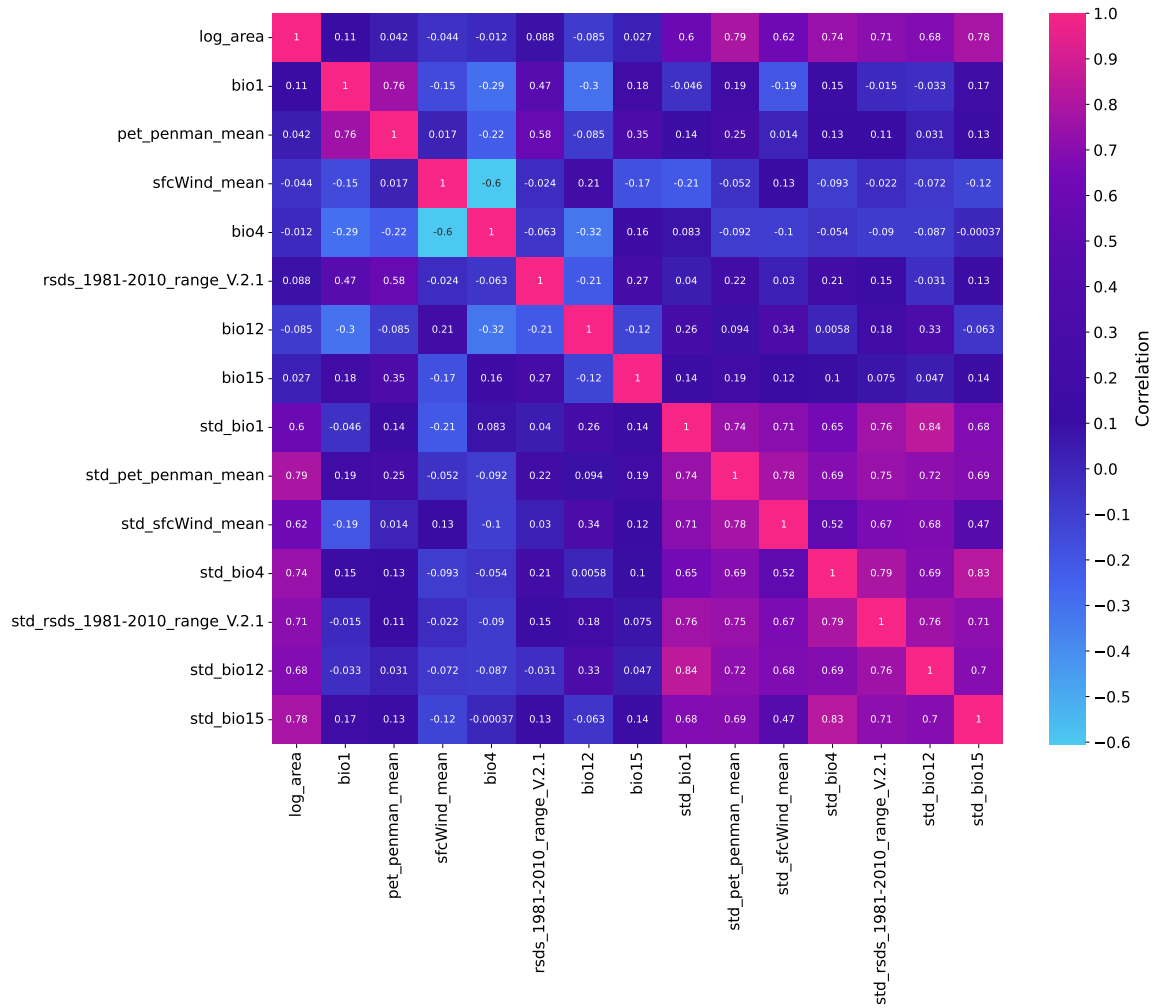


Figure S3: Correlation matrix of environmental features associated to the EVA-dataset.

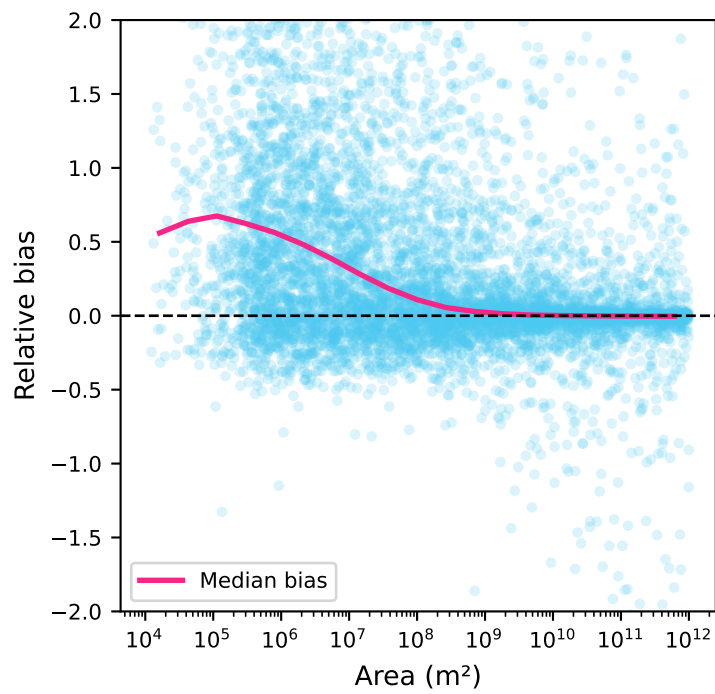


Figure S4: Relative bias of the deep SAR model on the EVA test dataset, calculated as the ratio of the difference between predicted and observed species richness to the observed species richness.

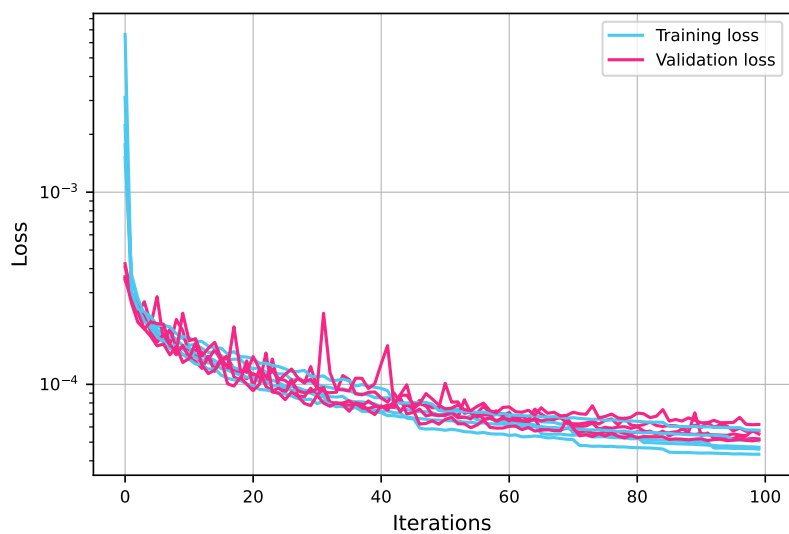


Figure S5: **Training and validation loss against the number of epochs for each member of the deep SAR ensemble model trained with area and climate features.**

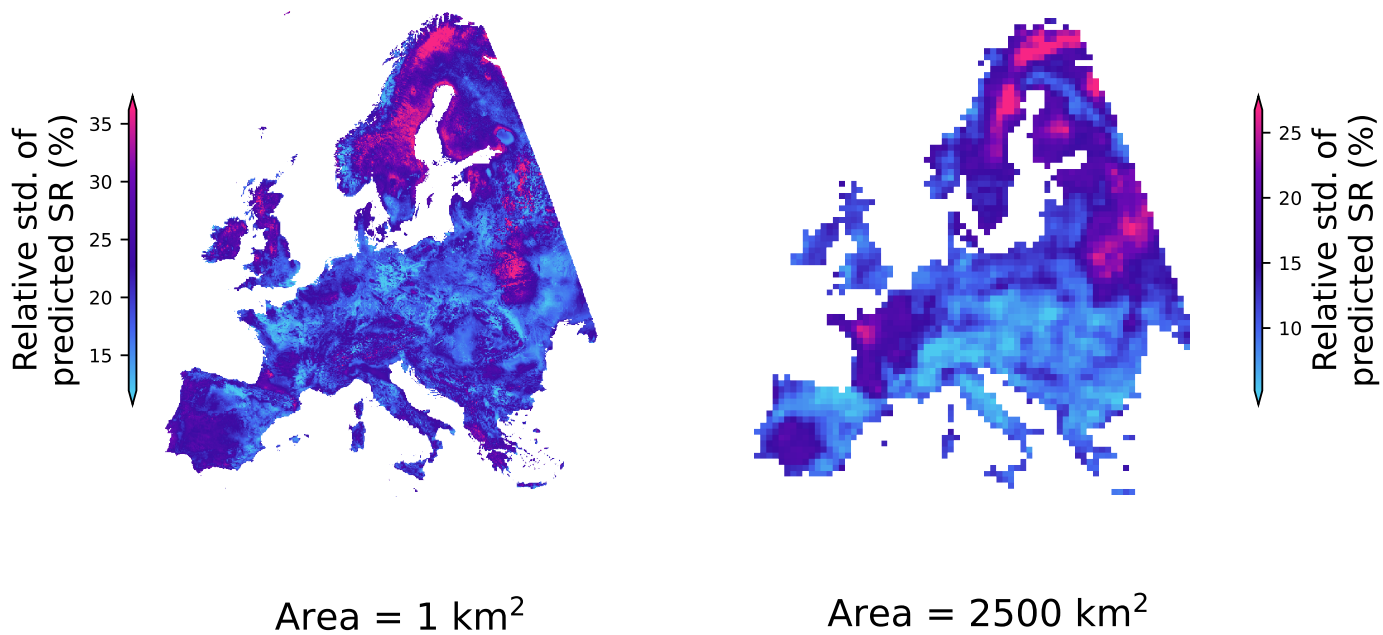


Figure S6: Relative standard deviation of the predictions obtained from the deep SAR ensemble model and displayed in Fig. 4.

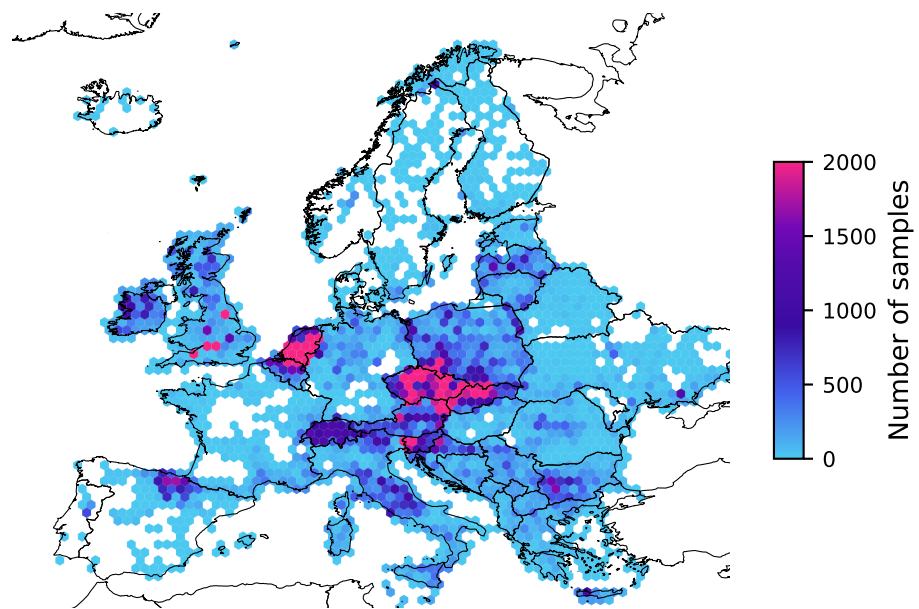


Figure S7: Density of EVA vegetation plots (number of samples per hexagon with width of 50km).